

**CONE BEAM COMPUTED TOMOGRAPHY IMAGING OF PERIODONTAL
BONE**

by
Ashok Balasundaram

A thesis submitted to the faculty of the University of North Carolina at Chapel Hill in partial fulfillment of the requirements for the degree of Master of Science in the Department of Diagnostic Sciences and General Dentistry, School of Dentistry.

Chapel Hill
2008

Approved by:

Advisor: Dr. Andre Mol, DDS, MS, PhD

Reader: Dr. Donald A. Tyndall, DDS, MSPH, PhD

Reader: Dr. John Moriarty, DDS, MS

ABSTRACT

Ashok Balasundaram: Cone beam Computed Tomography imaging of periodontal bone (Under the direction of Dr. André Mol)

Cone beam computed tomography (CBCT) is a low-dose, low-cost three dimensional imaging modality used for several oral and maxillofacial applications. This project evaluated the accuracy of Cone-Beam CT imaging to assess periodontal alveolar bone.

In Phase I, ground truth measurements of periodontal bone were obtained using *invitro* skull models. 146 sites were selected. Skulls were scanned with a CBCT unit and measurements from CT slices were obtained.

In Phase II, the diagnostic performance of the CBCT system was assessed compared to that of a full-mouth radiographic examination (FMX).

Measurements were compared to ground truth and A_z values were calculated from Receiver Operating Characteristic (ROC) curves. Analysis of Variance and Tukey's post-hoc test were used. The A_z -value for CBCT was 0.74 (SE=0.02) and for FMX 0.48 (SE=0.02). The difference was significant (ANOVA: $p < 0.01$).

CT images from NewTom Cone-beam CT scanner provided better diagnostic and quantitative information of periodontal bone than full mouth radiographs.

TABLE OF CONTENTS

List of Tables	v
List of Figures	vii
List of Abbreviations	ix
I. Introduction.....	1
II. Manuscript: IN VITRO CONE BEAM CT IMAGING OF PERIODONTAL BONE	
Abstract	8
Introduction.....	9
Materials and Methods	11
Image acquisition.....	12
Image viewing.....	13
Data Analysis.....	14
Results	15
Discussion	17
References	20
III. Appendix 1	
Materials and Methods	22
Description of Cone Beam CT scanner	22
Experimental design	24
Phase I	24
Ground truth	24
Phase II	26

Viewing sessions	27
IV. Appendix 2	
Protocol for observers – CBCT Images	28
Protocol for observers – Full Mouth X-rays.....	31
Results	33
Discussion	36
References	64

LIST OF TABLES

Table

1.	Distribution of sample sites by tooth group, site location and amount of bone loss.....	39
2.	Bone loss detection accuracy as measured by A_z (ROC analysis) for each modality and tooth group	40
3.	Absolute differences between ground truth measurements and image measurements by modality and tooth group	41
4.	Kappa values for intra-observer agreement between repeated ROC scores from bone loss assessment.....	42
5.	Area under the ROC curve (A_z) by modality, observer and Group	43
6.	Descriptive statistics for actual and absolute differences between ground Truth and CBCT image measurements (Phase I).....	44
7.	Results of ANOVA statistics on actual differences between ground truth and CBCT image measurements	45
8.	Results of ANOVA statistics on A_z values	46
9.	Summary of average differences between ground truth and CBCT, FMX measurements.....	47
10.	Tooth group wise distribution of absolute differences between CBCT and FMX modalities	48
11.	ANOVA results with significant interactions	49

12.	Pearson correlation coefficients for ground truth and image measurements by modality and tooth group.....	50
-----	---	----

LIST OF FIGURES

Figure

1.	Graph showing toothwise distribution of absolute and actual differences between CT and ground truth measurements	51
2.	ROC curves for pooled Az of two modalities (CBCT vs. FMX) for detection of periodontal bone loss	52
3.	ROC curves for Molar, Premolar and Anterior tooth groups (Modality: CBCT)	53
4.	ROC curves for Molar, Premolar and Anterior tooth groups (Modality: FMX).....	54
5.	Scatter plot with Pearson correlation for CBCT Anterior tooth group	55
6.	Scatter plot with Pearson correlation for FMX Anterior tooth group	56
7.	Scatter plot with Pearson correlation for CBCT Molar tooth group.....	57
8.	Scatter plot with Pearson correlation for FMX Molar tooth group.....	58
9.	Scatter plot with Pearson correlation for CBCT Premolar tooth group	59
10.	Scatter plot with Pearson correlation for FMX Premolar tooth group	60
11.	NewTom CBCT image slice of a lower lateral incisor tooth and corresponding lateral incisor periapical radiograph.....	61
12.	NewTom CBCT image slice of a lower molar tooth	

	and corresponding molar periapical radiograph	62
13.	NewTom CBCT image slice of a upper premolar tooth and corresponding premolar periapical radiograph	63

LIST OF ABBREVIATIONS

AEC	Automatic Exposure Control
ANOVA	Analysis of Variance
CEJ	Cementoenamel Junction
CT	Computed Tomography
CBCT	Cone Beam Computed Tomography
FMX	Full mouth X-ray
GT	Ground Truth
JFIF	JPEG File Interchange Format
JPEG	Joint Photographers Expert Group
PSP	Photostimulable Phosphor
ROC	Receiver Operating Characteristic
TACT	Tuned Aperture Computed Tomography

Introduction

Periodontal disease is a process which affects the supporting structures of the teeth (White & Pharoah, 2004). A gingival sulcus depth of more than 2 or 3 mm from the gingival margin is considered threshold for pocket formation (Hansen, Gjermo, & Bergwitz-Larsen, 1984). A periodontal pocket greater than 3 mm is considered pathologic (Davies, Downer, & Lennon, 1978; Hull, Hillam, & Beal, 1975). Periodontal disease is classified into slight, moderate and severe according to the severity of the underlying pathologic process (Armitage, 2004). Slight periodontitis indicates a pocket depth of 1-2 mm, moderate periodontitis, 3-4 mm and severe periodontitis, depth greater than 5 mm. Progressive spread of infection from the periodontal fibers destroys bone and renders teeth mobile and non-functional. Recent epidemiologic surveys reveal that chronic periodontitis is found in 30% of the population on an average of 3 to 4 teeth with periodontal pocket depths greater than 4 mm (Oliver, Brown, & Loe, 1998).

Diagnosis of periodontal disease is essential to formulate an effective treatment plan which, in turn, affects treatment outcome (Armitage, 2004). A thorough history, clinical examination and radiographic examination are important to establish a periodontal diagnosis. Radiographs play an essential adjunctive role in the diagnostic process (Armitage, 2004; Herzog & Paarmann, 1997). Radiographic examination of periodontal bone is used to assess the degree and pattern of bone loss with respect to the cemento

enamel junction. An ideal radiographic modality to image the periodontium would be one that produces an x-ray beam perpendicular to the image receptor. This would generate an image with the least distortion (Jeffcoat, Wang, & Reddy, 1995). At present, the modalities that best satisfy these requirements are periapical radiography and bitewing radiography (Pepelassi & Diamanti-Kipiotti, 1997). Periapical images are used to obtain a clear view of calculus, overhanging restorations, furcation defects and lesions in the apical periodontium. Bitewing radiographs are routinely used to obtain the best view of early interproximal and vertical bone loss (Tugnait, Clerehugh, & Hirschmann, 2000). Panoramic images give an overall impression of the maxillary and mandibular dentition and the surrounding alveolar bone. They serve as screening radiographs and are usually supplemented with periapical films (Akesson, Hakansson, & Rohlin, 1992). In some instances, panoramic images are used to view the periodontium. This compromises the visualization of alveolar bone due to the limited resolution and blurring of structures of interest.

Images obtained from conventional radiographic modalities are two dimensional representations of three dimensional anatomy (Jeffcoat et al., 1995; Mol, 2004). As a result of the collapse of structures on an image, the view obtained is unclear, distorted and suffers from magnification. Linear measurements from conventional radiographs frequently underestimated bone loss compared to clinical probing. Kilic AR et al. reported that the difference between probing bone loss and radiographic analysis was within one millimeter (Kilic, Efeoglu, Yilmaz, & Orgun, 1998). Also the correlation

between clinical probing and radiographic bone loss decreased as a function of time. Studies have reported a statistically significant correlation of 0.73 which reduced to 0.07 over a period of one year (Hausmann, 2000). Linear measurements have also been attempted on digitized radiographs and on serial radiographs using stored regions of interest in a computer (Benn, 1992). Though these digital methods reduced the difference in measurement between clinical probing and radiographic bone loss compared to direct measurement on conventional radiographs, the modalities used to obtain these digital images were still two-dimensional and suffered from inherent drawbacks (Benn, 1992; Hausmann, 1990; Hausmann, Allen, Carpio, Christersson, & Clerehugh, 1992; Hausmann, 2000).

Subtraction radiography is a specialized radiographic technique used to assess periodontal bone loss by comparing serial radiographs (H. G. Grondahl & Grondahl, 1983). It has been shown that even a 5% change in mineral bone loss can be detected by this technique (Ortman, Dunford, McHenry, & Hausmann, 1985). In assessing periodontal bone changes with this technique, it is essential that the x-ray beam geometry be nearly identical whenever two images are compared. (H. G. Grondahl & Grondahl, 1983; K. Grondahl, Grondahl, & Webber, 1984) Studies have reported various digital methods to produce a nearly identical geometry to compare images, which was difficult to establish earlier. Though the process of obtaining identical geometry for images taken over a period to time is getting better, the time and effort spent to produce images for use by this technique precludes its clinical use.

There is a need for a clear and undistorted view of the periodontal structures to make an accurate diagnosis and evaluate periodontal bone changes over a period of time. This would require the use of a three dimensional modality which would also enable making accurate and reproducible linear measurement of the alveolar bone on a 1:1 ratio (Kobayashi, Shimoda, Nakagawa, & Yamamoto, 2004; Van der Stelt, 1993; Vannier, 2003). Imaging modalities presently available to generate cross sectional images include Computed Tomography (CT) and Tuned Aperture Computed Tomography (TACT) (Ames, Johnson, & Stevens, 1980).

The routine application of CT for periodontal tissues is currently not indicated, because the risks associated with radiation absorbed dose for the patients do not outweigh the benefits of the information obtained (Ekestubbe, Thilander, Grondahl, & Grondahl, 1993; Fuhrmann, Bucker, & Diedrich, 1995; Fuhrmann, Wehrbein, Langen, & Diedrich, 1995; Naito, Hosokawa, & Yokota, 1998; Pistorius, Patrosio, Willershausen, Mildenerger, & Rippen, 2001; Rothman, Chaftez, Rhodes, & Schwarz, 1988; Webber, Horton, Tyndall, & Ludlow, 1997). Also, measurements of alveolar bone height in furcation areas from CT images overestimated bone loss by 4 mm or more (Pistorius et al., 2001).²⁵ Moreover, CT scanners are not available in a dental setting and the cost of obtaining and reformatting a scan is prohibitive. Resolution is also a limiting factor with reformatted CT images. TACT is an imaging modality that occupies the spectrum between transmission radiography and computed tomography (Webber et al., 1997; Webber & Messura, 1999). Studies have been done to assess the performance of TACT for various diagnostic

applications, including detection and localization of simulated periodontal defects (Ramesh, Ludlow, Webber, Tyndall, & Paquette, 2001). TACT enables the isolation of the structure of interest, limited to certain depths in the radiographed volume, by focusing the radiographic information derived from prerecorded projection data. With TACT there is no need to constrain associated projection geometry during the acquisition, which means that stringent patient positioning is not necessary between exposures. The three dimensional images and the number of possible angulation changes that can be made is limited.

A Dental CT technology, Cone Beam CT, is a modality recently developed and its applications are being explored in the maxillofacial region (Araki et al., 2004; Cho, Johnson, & Griffin, 1995; Danforth, Dus, & Mah, 2003; Hashimoto et al., 2003; Mozzo, Procacci, Tacconi, Martini, & Andreis, 1998; Sukovic, 2003). CBCT differs from conventional fan beam CT technique in its acquisition process. The x-ray beam is cone-shaped, while that of the conventional CT is fan-shaped. The scanning process in CBCT involves a single rotation of the x-ray source. The image reconstruction process is similar to that of conventional CT. The advantages of cone beam geometry include simplified design and a reduced patient dose. The effective dose from a cone beam scanner is approximately four times greater than that of a panoramic radiograph and forty-five times less than conventional CT doses (Ludlow, Davies-Ludlow, & Brooks, 2003; Schulze, Heiland, Thurmann, & Adam, 2004; S. C. White, 1992). CBCT is currently used for pre-surgical assessment of implant sites⁴³, orthodontics, pathoses and TMJ related disorders (Danforth,

Peck, & Hall, 2003; Hatcher, Dial, & Mayorga, 2003; Mozzo et al., 1998; Tsiklakis, Syriopoulos, & Stamatakis, 2004). Its potential application in evaluating periodontal bone loss is the focus of this investigation. The purpose of this study is to assess whether CBCT can overcome the limitations of conventional radiography in evaluating periodontal bone loss and estimate the difference in the accuracy of measurements from the two imaging modalities (Mol, 2004).

MANUSCRIPT

In Vitro Cone-beam CT Imaging of Periodontal Bone

Abstract

Objectives: To assess the accuracy of NewTom cone-beam CT (CBCT) images for the detection and quantification of periodontal bone defects in three dimensions.

Methods: A sample of 146 sites in five dry skulls provided the ground truth (GT). Half of the sample had bone loss of at least 3 mm. Two metal spheres at each site ensured correspondence between GT and CBCT measurements. Skulls were submerged in water and scanned with the NewTom QR-DVT-9000. A full mouth series (FMX) was obtained of each skull using photostimulable phosphor plates. Six observers measured bone height of each site and rated the presence or absence of bone loss. Measurements were compared to GT and A_z -values were calculated from Receiver Operating Characteristic curves.

Results: The A_z -value for CBCT was 0.74 (SD=0.14) and for FMX 0.48 (SD=0.09). The difference was significant (ANOVA: $p < 0.01$). The diagnostic accuracy of CBCT was lower for anterior teeth ($A_z=0.59$) than for molars ($A_z=0.82$) and premolars ($A_z=0.79$) (Tukey HSD: $p < 0.01$). The mean absolute difference between CBCT and GT was 1.27 mm (SD=1.43) and between FMX and GT 1.49 mm (SE=1.24) (ANOVA: $p < 0.01$). Measurements in the anterior mandible were less accurate than in other areas (Tukey HSD: $p < 0.01$).

Conclusion: The NewTom cone-beam CT scanner provides better diagnostic and quantitative information on periodontal bone levels in three dimensions than conventional radiography. The accuracy in the anterior aspect of the jaws is limited.

Introduction

Two basic elements of a periodontal diagnosis are the severity of the problem and whether the condition is localized or generalized (Armitage, 2004).

Radiography plays an important adjunctive role in periodontal diagnosis primarily by providing information regarding the amount and type of damage to the alveolar bone (Armitage, 2004; Mol, 2004). While radiographs also reveal related issues, such as calculus and defective restorations, assessment of alveolar bone height with respect to the cemento-enamel junction is the main outcome of a radiological examination in support of a periodontal diagnosis.

Conventional modalities commonly used for assessing alveolar bone height include bitewing, periapical and panoramic radiography (Akesson, Hakansson, & Rohlin, 1992; Jeffcoat, Wang, & Reddy, 1995; Mol, 2004; Tugnait, Clerehugh, & Hirschmann, 2000). The bitewing technique is the conventional modality that is best suited for assessing bone height, because it approaches ideal projection geometry and shows both mandibular and maxillary structures (Eley & Cox, 1998; Hausmann, 1990; Mol, 2004; White et al., 2001). However, all conventional modalities produce two-dimensional images that collapse the three-dimensional structures based on differential attenuation of x-rays. Thus, important aspects of the alveolar bone may go undetected as a result of an unfavorable location with respect to other structures or an unfavorable orientation with respect to the x-ray beam. Only the interproximal bone levels can be detected with some level of certainty (Mol, 2004). Even when high quality images are produced, intraoral

radiographs have been shown to underestimate mild to moderate bone loss (Akesson et al., 1992; Eickholz & Hausmann, 2000; Pepelassi & Diamanti-Kipiotti, 1997; Tonetti, Pini Prato, Williams, & Cortellini, 1993).

Subtraction radiography, by virtue of its highly standardized acquisition technique and precise analytical methods, has shown to be more accurate and to allow for earlier detection of osseous changes than conventional radiography (Mol & Dunn, 2003; Ortman, Dunford, McHenry, & Hausmann, 1985; Reddy & Jeffcoat, 1993). However, this technique is labor intensive and does not have the capability to provide accurate 3D information either. The inherent limitations of conventional radiography result in incomplete and imprecise assessment of the condition of the alveolar bone.

The ability to visualize the alveolar bone in three dimensions and make measurements at any location has the potential to significantly improve periodontal diagnosis. The modality that is best suited for 3D imaging of mineralized tissues is computed tomography (CT). Studies have shown that assessment of alveolar bone height on CT images is reasonably accurate and precise. However, medical CT examinations are dose intense and have an unfavorable cost-benefit ratio for periodontal purposes.

These drawbacks have largely been overcome with the development of cone-beam CT (CBCT) scanners. CBCT scanners are specifically designed for imaging the hard tissues of the head and neck. They are much cheaper than medical CT units, impart a relatively low dose to the patient (Ludlow, Davies-

Ludlow, Brooks, & Howerton, 2006), and are becoming rapidly available to the dental profession. It is the purpose of this study to assess the usefulness of CBCT for the assessment of alveolar bone loss and compare its diagnostic performance with periapical and bitewing radiography *in vitro*. The specific aims of this study are to assess the diagnostic efficacy of cone-beam CT images for the detection of alveolar bone loss and to determine the accuracy of quantitative measurements of alveolar bone height in 3D.

Materials and Methods

Five dentate dry skulls were selected to provide the periodontal ground truth (GT) model. The sample consisted of 146 sites stratified according to tooth group and site location. Six tooth groups were identified: upper molar (UM), upper premolar (UP), upper anterior (UA), lower molar (LM), lower premolar (LP) and lower anterior (LA). The actual measurement sites were classified as mesiobuccal (MB), buccal (B), distobuccal (DB), mesiolingual (ML), lingual (L) and distolingual (DL). Based on a bone loss threshold of 3 mm, half of the sample was “healthy” (median = 2.4 mm; inter-quartile range (IQR) = 0.5 mm) and the other half showed bone loss (median = 4.2 mm; IQR = 1.3 mm). Table I shows the distribution of the sites per tooth group and site location.

Two small metal spheres were attached to the crown of the tooth at each site to mark the exact location and orientation of each measurement.

Measurement of the distance between the cemento-enamel junction and the alveolar crest was performed according to the line connecting the spheres.

Skull measurements were made by a single examiner using a digital caliper

with a resolving capacity of 0.1 mm. The average of three measurements was considered the ground truth value.

Image acquisition

The skulls were scanned with the NewTom QR-DVT-9000 CBCT unit (QR-NIM s.r.l., Verona, Italy). Scans were performed with the skulls submerged in water to provide adequate x-ray attenuation and scattering. Exposure parameters were selected automatically by the scanner based on the attenuation properties of each skull. Primary reconstruction of the raw data resulted in axial slices parallel to the occlusal plane with a slice thickness of 0.3 mm. For those skulls that exhibited a deep curve of Spee, multiple primary reconstructions were performed to yield axial images that were locally parallel to the occlusal plane for each region of interest.

Cross-sectional slices of 1 mm thickness were constructed from the axial slices for each site. The slice location and orientation was dictated by the metallic markers such that both markers were visible in the slice (Figure 1). This ensured correspondence between slice measurements and ground truth measurements.

A series of fourteen periapical and four horizontal bite-wing radiographs (FMX) was obtained of each skull using photostimulable phosphor (PSP) plates. The plates were scanned with the Gendex DenOptix scanner at 300 dots per inch and stored as 8 bit JFIF(100) images.

Image Viewing

CBCT image slices were exported from the NewTom software in bitmap format. Gendex PSP images were exported in JPEG (Joint Photographers Expert Group) format. Images from both modalities were then imported into Schick CDR software (Schick Technologies, Inc., Long Island City, NY). Both sets of images were spatially calibrated according to known dimensions of the native images. A magnification factor of 1.05 was used for all intraoral images. Four board-certified oral and maxillofacial radiologists, one oral and maxillofacial radiology resident and one periodontist were recruited as observers. The observers were calibrated using a training session. The observers were asked to measure the distance between the cemento-enamel junction and the alveolar crest for each site and each modality using the Schick CDR length measurement tool. Based on a bone loss threshold of 3 mm, they were also asked to assess the presence or absence of bone loss (vertical or horizontal) on a five-point scale as follows: 1 = bone loss definitely absent, 2 = bone loss probably absent, 3 = uncertain, 4 = bone loss probably present, 5 = bone loss definitely present.

The observations were performed in seven separate sessions: three CBCT sessions, three FMX sessions and one combined CBCT-FMX repeat session. The order in which the two modalities were viewed was reversed for half of the observers to minimize order effects. The presentation of the images within and among sessions was random. The repeat session included a 20% random sample from the main sessions.

Data Analysis

CBCT and FMX measurements were compared to ground truth measurements using ANOVA statistics. Since positive and negative differences cancel each other out, analysis was performed on the absolute differences. Actual differences were considered only to determine the direction of the differences. The main effects of modality, tooth group, site and observer were tested along with the interactions. Tukey's HSD post-hoc test was used to determine significant differences within groups.

Diagnostic accuracy of determining the presence or absence of bone loss was assessed using Receiver Operating Characteristic (ROC) curves. The area under the curve (A_z) was calculated for each combination of observer, modality and tooth group using ROCKIT 0.9B (Charles Metz, University of Chicago, Chicago, IL). Differences between areas under curves (A_z) were analyzed using ANOVA ($\alpha = 0.05$).

Intra-observer agreement for bone loss assessment was determined by comparing ROC scores of repeated observations. The kappa statistic with linear weighting was used to account for chance agreement (VassarStats, Richard Lowry, Vassar College, Poughkeepsie, NY).

Results

The results of the ROC analysis are presented in Table 2 and Figures 2, 3 and 4. Analysis by tooth group resulted in degenerate data making it necessary to collapse the original six tooth groups into three (molars, premolars and anterior teeth). Analysis of variance showed that differences between observers were not statistically significant ($p = 0.69$), but differences between modalities ($p < 0.0001$), tooth groups ($p = 0.01$) and the interaction between modality and tooth group ($p = 0.01$) were. Tukey's HSD post-hoc test shows that CBCT was significantly better than FMX for the molar and premolar tooth groups. The diagnostic accuracy of CBCT in the anterior region was not significantly different from the diagnostic accuracy of FMX.

The average difference between ground truth measurements and CBCT measurements was -0.23 mm. This implies that there was slightly more underestimation than overestimation of bone loss. For FMX, the average actual difference was -1.17 mm, also implying more underestimation than over estimation of bone loss. The real difference between ground truth measurements and image measurements is better described by the absolute difference. While this measure does not account for the direction of the error, it prevents positive and negative errors to cancel each other out. Absolute differences between ground truth measurements and measurements from either of the two imaging modalities are summarized in Table 3. Overall, CBCT measurements were more accurate than FMX measurements ($p < 0.0001$). There was no significant difference between observers. Tooth group differences were significant ($p < 0.0001$). Table 3 also shows the homogenous

subsets based on Tukey's post hoc test. The measurement error for the lower anterior (LA) teeth was significantly larger than for the other tooth groups for both modalities. The interaction between modality and tooth group was not statistically significant.

Kappa values representing intra-observer agreement for bone loss assessment are shown in Table 4. Overall, both modalities resulted in slight agreement, with only two observers showing fair agreement (Landis & Koch, 1977).

Discussion

The purpose of this study was to assess the usefulness of CBCT for the assessment of alveolar bone loss and compare its diagnostic performance with periapical and bitewing radiography. The results show that the accuracy of detecting bone loss was significantly better with CBCT than with conventional intraoral radiographs. This was true only for posterior teeth. The diagnostic accuracy of both imaging modalities was low for anterior teeth. The difference in the diagnostic accuracy of CBCT between anterior and posterior teeth is likely the result of the difference in the morphology of the periodontal bone between these areas. The buccal and lingual plates are considerably thinner in the anterior region and the bone tapers towards the crest. Apparently, the quality of the CBCT image slices is insufficient to resolve the alveolar crest reliably in this region.

The inclusion of buccal and lingual sites in the sample created a bias in favor of CBCT as it is known that bone levels in these areas are very difficult to visualize with intraoral radiographs. The inclusion of these sites demonstrated the capability of three-dimensional imaging to visualize bone levels in areas where conventional modalities fall short. The sample was somewhat unbalanced because of the relatively large number of buccal sites. It should also be noted that the bias against conventional radiography was further increased by the fact that proximal sites were not absolutely mesial or distal. The selection of these sites was dictated by the need to obtain reliable ground truth measurements without destroying the sample. Considering these

limitations, conventional radiography simply served as a control, confirming that 3D information cannot be obtained with traditional means.

Despite the higher diagnostic accuracy of CBCT, bone height measurements were only slightly better than those for conventional radiography. Both modalities resulted in average measurement errors larger than 1 mm. This appears a clinically significant error requiring improvement.

Whereas CBCT was better than conventional radiography both in terms of diagnostic and quantitative accuracy, it was by no means perfect. It is known that perception errors are inherent to human observations and decisions, however, the magnitude of the error in visual perception is modulated by image clarity. The CBCT scans used in this study sometimes lacked image clarity, which was especially apparent in areas where diagnostic decisions were determined by small details. Lack of image clarity can be the result of limited spatial resolution, limited contrast resolution, poor signal-to noise ratio (SNR) or a combination of these. The voxel size of approximately 0.3 mm suggests that CBCT could be useful for periodontal imaging. However, the cemento-enamel junction and, in some instances, the coronal edge of the alveolar bone are defined by tapering structures, which may challenge the spatial resolution of the system. Apart from voxel size, spatial resolution is also modulated by SNR, which may have been a key factor limiting the detection rate.

It should be emphasized that current results were obtained with an early generation CBCT scanner, which is no longer available. Recent advances in CBCT technology suggest that the current scanners, including the NewTom 3G, are likely to exceed the results obtained in this study. Improvements include increased contrast resolution through higher bit depth (from 8 to 12 bits), better SNR and higher spatial resolution. These developments and the results of this study support further investigation of the usefulness of CBCT for periodontal diagnosis to increase accuracy and expand periodontal bone height assessment beyond the traditional mesial and distal locations.

From the results of this study it can be concluded that the NewTom 9000 cone-beam CT scanner provides better diagnostic and quantitative information on periodontal bone levels than conventional radiography. The accuracy in the anterior aspect of the jaws is limited.

References

1. Akesson, L., Hakansson, J., & Rohlin, M. (1992). Comparison of panoramic and intraoral radiography and pocket probing for the measurement of the marginal bone level. *Journal of Clinical Periodontology*, 19(5), 326-332.
2. Armitage, G. C. (2004). The complete periodontal examination. *Periodontology 2000*, 34, 22-33.
3. Eickholz, P., & Hausmann, E. (2000). Accuracy of radiographic assessment of interproximal bone loss in intrabony defects using linear measurements. *European Journal of Oral Sciences*, 108(1), 70-73.
4. Eley, B. M., & Cox, S. W. (1998). Advances in periodontal diagnosis. 1. traditional clinical methods of diagnosis. *British Dental Journal*, 184(1), 12-16.
5. Hausmann, E. (1990). A contemporary perspective on techniques for the clinical assessment of alveolar bone. *Journal of Periodontology*, 61(3), 149-156.
6. Jeffcoat, M. K., Wang, I. C., & Reddy, M. S. (1995). Radiographic diagnosis in periodontics. *Periodontology 2000*, 7, 54-68.
7. Landis, J. R., & Koch, G. G. (1977). The measurement of observer agreement for categorical data. *Biometrics*, 33(1), 159-174.
8. Ludlow, J. B., Davies-Ludlow, L. E., Brooks, S. L., & Howerton, W. B. (2006). Dosimetry of 3 CBCT devices for oral and maxillofacial radiology: CB mercuray, NewTom 3G and i-CAT. *Dento Maxillo Facial Radiology*, 35(4), 219-226.
9. Mol, A. (2004). Imaging methods in periodontology. *Periodontology 2000*, 34, 34-48.
10. Mol, A., & Dunn, S. M. (2003). The performance of projective standardization for digital subtraction radiography. *Oral Surgery, Oral Medicine, Oral Pathology, Oral Radiology, and Endodontics*, 96(3), 373-382.
11. Ortman, L. F., Dunford, R., McHenry, K., & Hausmann, E. (1985). Subtraction radiography and computer assisted densitometric analyses of standardized radiographs. A comparison study with 125I absorptiometry. *Journal of Periodontal Research*, 20(6), 644-651.
12. Pepelassi, E. A., & Diamanti-Kipioti, A. (1997). Selection of the most accurate method of conventional radiography for the assessment of periodontal osseous destruction. *Journal of Clinical Periodontology*, 24(8), 557-567.

13. Reddy, M. S., & Jeffcoat, M. K. (1993). Digital subtraction radiography. *Dental Clinics of North America*, 37(4), 553-565.
14. Tonetti, M. S., Pini Prato, G., Williams, R. C., & Cortellini, P. (1993). Periodontal regeneration of human infrabony defects. III. diagnostic strategies to detect bone gain. *Journal of Periodontology*, 64(4), 269-277.
15. Tugnait, A., Clerehugh, V., & Hirschmann, P. N. (2000). The usefulness of radiographs in diagnosis and management of periodontal diseases: A review. *Journal of Dentistry*, 28(4), 219-226.
16. White, S. C., Heslop, E. W., Hollender, L. G., Mosier, K. M., Ruprecht, A., Shrout, M. K., et al. (2001). Parameters of radiologic care: An official report of the american academy of oral and maxillofacial radiology. *Oral Surgery, Oral Medicine, Oral Pathology, Oral Radiology, and Endodontics*, 91(5), 498-511.

Appendix 1

Materials and Method

Description of Cone Beam CT Scanner

The CBCT scanner used in this study was the NewTom DVT 9000 (QR- NIM s.r.l., Verona, Italy). This scanner is dedicated to image the maxillofacial region. The NewTom CBCT scanner works on the principle of cone beam technology which is one of the three-dimensional imaging dental CT technologies available at present with a reduced dose to the patient compared to conventional CT technology.

Scanning with the NewTom QR-DVT 9000 involves a single rotation of the x-ray source through 360 degrees to generate a scan of the entire head in the shape of a cone. This produces 360 basis images (one projection for every degree). The total exposure time is 36 seconds with an effective exposure time of 18 seconds. A typical scan requires an exposure of 3.2 mA and 100 kVp. The scanner has an automatic exposure control (AEC) mechanism that calculates the starting intensity and also any change in intensity during the scan. Wedge shaped filters are used to modulate the intensity of the beam to produce a circular field of view.

The x-ray detector system consists of an image intensifier containing a solid state Charge Couple Device (CCD) detector. The CCD detector has a matrix size of 512 x 512 pixels. The entrance screen of the image intensifier is approximately 400 sq.cm. The reconstruction volume is spherical with a

diameter of approximately 15 cm.³⁵ The raw data obtained from the scan is corrected for geometric and dynamic distortions prior to the primary reconstruction process. Primary reconstruction is done by a 3-D filtered back projection method proposed by Feldkamp et. al. Primary reconstruction from the raw data result in the formation of all axial slices from the region selected by the operator on one of the lateral scout views. Axial slices are 0.3 mm thick. Several primary reconstructions can be obtained on different planes from a single scan. Secondary reconstruction involves the reformatting of axial slices obtained from Primary reconstruction of raw data. This results in the production of slices perpendicular to the dental arch and panoramic images along the plane of the arch. Cross-sectional images are usually 1 mm thick. Features available in the software include: (1) measurements with the use of the mouse and (2) colored marker to point an anatomic detail on a 2-D view and recover it on all reformatted slices.³⁵

CBCT is an evolving imaging technology for three-dimensional evaluation of the maxillofacial region. NewTom QR-DVT 9000 is a CBCT scanner. The scanner works on cone beam technology compared to the fan-beam used in a conventional fan beam CT scanner. The spatial resolution of this scanner is 0.3 mm. The potential limitations of this scanner include :(1) scattered radiation which exaggerates noise in the image and reduces SNR (signal to noise ratio); (2) truncated-view artifact produced with a fully open field-of-view. This can be easily reduced by visualizing a smaller field of view; (3) contrast resolution is low; and (5) soft tissue imaging is not possible.³⁵

Experimental design

The general design of this study was based on comparing cone beam CT images based on their qualitative features and quantitative ground truth measurements. The first phase of the study was designed to establish ground truth measurements on dry skulls and to verify measurement accuracy and measurement reproducibility on images obtained with the NewTom CT scanner. The second phase was designed to assess diagnostic efficacy. Specifically, the ability of observers to detect the presence or absence of alveolar bone was tested and their measurements on the CT and full mouth radiographic images were compared to established ground truth values.

Phase I

Ground truth

Five dentate dry skulls were randomly selected. The skulls showed varying bone levels throughout their dentitions required for this study. No artificial bony lesions were created. The teeth in each skull were divided into groups i.e. Upper molar, Upper premolar, Upper anterior, Lower molar, Lower premolar and Lower anterior. The surfaces around the teeth to be studied were designated as “sites” and further classified into Buccal, Mesiobuccal, Distobuccal, Lingual, Distolingual and Mesiolingual. Based on a bone loss threshold of 3 mm, half of the sample was healthy (median = 2.4 mm; inter-quartile range (IQR) = 0.5 mm) and the other half showed bone loss (median = 4.2 mm; IQR = 1.3 mm). Table I shows the distribution of the sites per tooth group and site location.

146 sites were selected by a randomization process. Prior to commencing the measurement procedure, it was essential to make sure the plane of measurement in the skull corresponds exactly to the plane being produced by the CT slice. This was accomplished as follows. Reference points were created by fixing two metallic spheres 0.75 mm in diameter on the crown corresponding to the site to be measured. The extension of an imaginary line connecting the two spheres would define the exact location of the site both on the skull and on the images of the CT slices.

Ground truth measurements were made on the selected sites using a calibrated digital caliper with a resolving efficiency of 0.1 mm. Three sets of measurements were made by a single examiner (A.B) and the average calculated. After establishing ground truth measurements, the skulls with the metallic spheres, were immersed in water, which acted as a scattering agent. All attempts were made to stabilize the skull in the container of water. Each skull to be scanned was placed in the gantry of the CT scanner. Any correction to the skull and table position prior to scanning was done after assessing the frontal and lateral aspects of the scout view. The collimator was opened to its fullest extent to encompass the maxilla and mandible. The scanning procedure was done with parameters described in the Appendix. The same procedure was repeated to scan the rest of the skulls used in the study. The cross-sectional images of the sites to be measured were secondarily reconstructed with the help of the software available in the NewTom scanner. The cross-sectional CT slices which identified the two metallic spheres were used for measurement. This made sure that the

reference plane in the image corresponded exactly to that of the plane in which the ground truth measurements were made. Three sets of measurements (CEJ- alveolar crest) were made by the same examiner and the average values calculated.

Phase II

The second phase of the study focused on the diagnostic accuracy of observers to interpret alveolar bone height. Also, the diagnostic efficacy of the CT images was compared to that of conventional full mouth radiographic images, as determined by observers. The purpose of this phase of the study was to assess the viability of this modality for use in a real clinical situation.

Cross-sectional CT images from each site to be viewed were exported from the NewTom software in Bitmap format. They were then imported into the Schick CDR Dicom software (Schick Technologies Inc.) which served as the interface software. The software allowed the observers to select each session containing a set of images and perform the scoring. 146 images with an equal number of negative and positive bone loss sites were included in the sessions.

Full mouth radiographic images to be viewed were made of the five skulls used in the study with the help of photostimulable phosphor plates (PSP). The Full mouth x-rays (FMX) consisted of fourteen periapical radiographs and four bitewing radiographs. The Full mouth radiographic series (FMX) was also made available for visualization in the Schick software. They were added to

CT images and the same sites that were selected for CT images were included in the FMX for scoring by the observers.

Viewing sessions

Six observers were selected. They included four board certified oral radiologists, an oral radiology graduate student and a periodontologist. All the observers were calibrated before the scoring sessions. All the images to be viewed were also calibrated. The observers graded the bone height using a five point rating scale (1=bone loss definitely absent, 2= bone loss probably absent, 3= undecided, 4= bone loss probably present, 5= bone loss definitely present). The observers were then asked to measure the alveolar bone height, in millimeters, from the cemento-enamel junction to the alveolar crest with the help of a measurement tool. The design of the viewing sessions included limiting the effect from the order of sessions. The effect would be that if all observers performed the same modality first, the second modality would consistently perform better by way of observers gaining information from the first modality. This would lead to a bias in the study. This effect was limited in our study by asking three observers to perform the CT viewing session first and the other three observers perform the FMX viewing session first. The observers then switched to the other modality after completion of the first modality which they had started with. This way bias, if any, would cancel out. A repeat session was arranged for all viewers comprising 20% of the images seen in the first session after a period of one week.


Appendix 2

Protocol for viewing sessions

CBCT Images

Dear observers,

Thank you for accepting to participate in this research study. The following protocol will serve as a guide to score the CT images in the study. While performing the scoring, please dim the room lighting and take a break when you feel the effects of fatigue.

1. Open the icon “CDR Dicom for Windows” from the desktop
2. Click the “Open” folder
3. Click “Search” on the patient query dialog box and this opens up and lists all the sessions
4. Double click on the session to be scored and these will open up all the images to be scored for that particular session
5. The CT “slices” or sites to be observed are numbered in a sequential descending order and the image no. appears on the “Comments” section of the “Exam information” situated above the image.
6. The CT “slices” or sites to be observed are numbered in a sequential descending order and the image no. appears on the “Comments” section of the “Exam information” situated above the image.
7. There is one image per tab and the image is oriented for the normal viewing mode.
8. Click on 
9. This leads to the first image to be scored.

10. The scoring sheet provided lists the tooth (upper/lower) and side of the image to be scored (left/right).
11. The tooth and side that are being scored should correspond to that in the scoring sheet.
12. To begin scoring, left click on the mouse once which will lead to a zoomed image overlapping the original image. This zoomed image is made use for brightness and contrast adjustment and making measurements.
13. The measurement from CEJ to alveolar crest is done with the help of the measurement tool.
14. To begin making a measurement, click the “measure” icon. Now, left click on the starting point to be measured and drag till the ending point to be measured and now release the left click. The selected length appears as a measured value on the image. Enter the value in millimeters (mm) in the corresponding area in the scoring sheet.
15. After entering the alveolar bone height, circle from the scale numbered from 1 to 5 by selecting the appropriate number for that image. The rating scale is as follows:
 1. Bone loss definitely absent
 2. Bone loss probably absent
 3. Undecided
 4. Bone loss probably present
 5. Bone loss definitely present
16. The criteria for assessment of bone loss is as follows:
 1. <3 mm = no bone loss
 2. > 3 mm = bone loss present

17. The same procedure is repeated until all the four sessions are completed.

Protocol for viewing sessions

Full Mouth Radiographs

Dear observers,

Thank you for accepting to participate in this research study. The following protocol will serve as a guide to score the full mouth radiographic images in the study. While performing the scoring, please dim the room lighting and take a break when you feel the effects of fatigue.

1. Open the icon “CDR Dicom for Windows” from the desktop
2. Click the “Open” folder
3. Click “Search” on the patient query dialog box and this opens up and lists all the sessions
4. Double click on the session titled “Full Mouth X-rays” to be scored and this will open up the full mouth series to be scored.
5. Each full mouth series is assigned a tab and is identified with the help of the “skull #” assigned in the “Comments” section under “Exam information”.
The full mouth series is oriented in the normal viewing mode.
6. The skull #'s under the “Comments” section should correspond to the skull #'s in the scoring sheet.
7. The skull #'s under the “Comments” section should correspond to the skull #'s in the scoring sheet.
8. Click in the appropriate intra-oral mount which represents the site to be scored. A red box appears on the mount selected.
9. After the site in the mount has been identified, left click once inside the mount.

10. This opens up the window to make brightness and contrast adjustments and make measurements to begin scoring.

11. The measurement from the CEJ to the alveolar crest is done with the help of the measurement tool. To begin making a measurement, click the “measure” icon. Now left click on the starting point to be measured and drag till the ending point to be measured and now release the left click. The selected length appears as a measured value on the image. Enter the value in mm in the corresponding area in the scoring sheet.

12. After entering the alveolar bone height, circle from the scale numbered from 1 to 5 by selecting the appropriate number for that image. The rating scale is explained as follows: (please try to use the full range of the scale while scoring)

1. Bone loss definitely absent
2. Bone loss probably absent
3. Undecided
4. Bone loss probably present
5. Bone loss definitely present

13. The criteria for assessment of bone loss are as follows:

1. < 3 mm = no bone loss
2. ≥ 3 mm = bone loss present

Results

The difference between ground truth measurements and image measurements is better described by the absolute difference. While this measure does not account for the direction of the error, it prevents positive and negative errors to cancel each other out.

Results of Phase I of the study indicate that the mean absolute difference between ground truth measurements and CBCT measurements as measured by a single examiner was less than 1 mm (0.85) (Table 6). The tooth group was a variable which showed a statistically significant difference (Table 7). The lower anterior tooth group particularly was different from the other tooth groups studied (Table 3). This could be due to the presence of thin cortical bone which makes identification of the crest difficult (Table 3, Fig.11a).

Results of Phase II of the study indicate that there was a difference in the A_z values between the CT and FMX as scored by the observers (Table 5, Fig.2). Analysis by tooth group resulted in degenerate data making it necessary to collapse the original six tooth groups into three (molars, premolars and anterior teeth). Differences in A_z among tooth groups in each of the modalities were noted. (Table 2, Fig.3, Fig.4). Anterior, Molar and Premolar tooth groups showed difference in A_z between the two modalities (Fig.3, Fig.4). The molar tooth group performed the best and the anterior tooth group the least with the CT modality. The premolar tooth group performed the best and the molar the least with the FMX modality.

The difference in diagnostic performance between CT and FMX was statistically significant (<0.0001) (Table 8). The pattern of overestimation continued even among tooth groups (Table 9). The diagnostic accuracy of CBCT in the anterior region was not significantly different from FMX for any of the tooth groups.

The average actual difference between ground truth measurements and CBCT measurements was -0.23 mm (Table 9). This implies that there was slightly more underestimation than overestimation of bone loss. For FMX, the average actual difference was -1.17 mm, also implying more underestimation than over estimation of bone loss (Table 9). The CT and Full mouth radiographic measurements overestimated the ground truth measurements by a mean of 1.276 and 1.485 respectively (Table 10). Absolute differences between ground truth measurements and measurements from either of the two imaging modalities are summarized (Table 10). Overall, CBCT measurements were more accurate than FMX measurements ($p < 0.0001$). There was no significant difference between observers.

From the ANOVA on absolute differences, supplementary results were obtained. Modality, observers and tooth group were statistically significant ($P < 0.0001$) (Table 11). Lower anterior tooth group and lingual surface were different from the rest of the tooth group and surfaces.

Pearson correlation co-efficient between ground truth measurements and measurements from the two modalities were low to moderate (Table 12).

Scatter plots of the absolute differences between ground truth measurements

and the two modalities, according to the tooth groups, are shown in Fig.5- Fig.10. Overall, both modalities resulted in slight agreement, with only two observers showing fair kappa values (Landis JR, Koch GG. The measurement of observer agreement for categorical data. Biometrics 1977; 33: 159-174). The correlation between repeated bone height assessments was low to moderate. Overall, CBCT measurements were slightly more reproducible than FMX measurements with considerable differences between observers.

Discussion

The limitations of two dimensional imaging for periodontal bone assessment are well understood. The need for a 3-D imaging modality for better assessment of periodontal bone is imminent. Conventional CT cannot be considered a viable alternative due to dose issues. There is still a need a for a low-cost, low-dose alternative to conventional CT to assess periodontal bone.

A CBCT volume produces substantial additional information compared to conventional radiography. With this concept in mind, a research design was constructed to compare the diagnostic accuracy of CBCT with conventional radiography to assess periodontal bone. The current study differs from a similar study with important modifications in the research design (Pinsky, Dyda, Pinsky, Misch, & Sarment, 2006). Our experiment used metallic markers on crowns of teeth to make sure reference planes for measurement were similar on the skull and the images produced. Also, the results of our study were based on naturally detectable periodontal bone and were not simulated defects as in the other study.

Results from this study indicated that diagnostic accuracy of CBCT ($A_z = 0.74$) was better than conventional radiography ($A_z = 0.48$). The difference in A_z was statistically significant. The difference in A_z values between the two imaging modalities continued onto the different tooth groups. A_z values for the molar and anterior tooth group in the CBCT modality was 0.82 and 0.59 respectively. This could be due to the increased sampling volume in molar teeth and thin buccal and lingual cortical plates in the anterior tooth group.

Thin cortical plates in the anterior teeth could have increased the difficulty of observers to identify the cemento-enamel junction and alveolar crest.

To be useful clinically, periodontal measurements need to be consistent over intervals of time (Hausmann & Allen, 1997). For example, in our study, the consistency of observers on repeated CBCT measurements was low. It is not known if more observers would have influenced results. Low Pearson correlation values (0.32) for repeated measurements with the CBCT images could be explained by the reduced image quality which led to poor correlation on similar sites. Correlation analysis for conventional full mouth radiographic measurements was expectedly low (0.24).

The assessment of periodontal bone through measurements preceded detection of bone loss. This emulates the clinical situation where measurements are obtained before diagnosis of periodontal health or disease is made. Actual and absolute measurements from this study showed that CBCT performed better than conventional radiography. However, both modalities overestimated bone height. These results differ from similar studies which found underestimation of bone height, particularly with conventional CT (Fuhrmann, Bucker, & Diedrich, 1995). The reason for the difference in results is not known. In another study with a NewTom CBCT scanner similar to the one used in this study, Lascala et al. found CBCT measurements to be lower than ground truth measurements (Lascala, Panella, & Marques, 2004). However, their study sample consisted of extra oral sites that did not include

the maxillary or mandibular teeth and so could not be directly compared to our study.

The results should also be judged in context of image quality and difference in dose between the two imaging modalities. If CBCT is to succeed as a clinical tool in periodontics, the accuracy in detecting cemento-enamel junction and alveolar crest should improve. Also, difference in bone height measurements between intervals of time should be as little as 0.5 mm (Benn, 1992). This can be achieved through improvements in image quality. There are indications that this may occur. Newer CBCT machines with technically efficient detectors are available which could increase image quality. With this improvement and consistency in measurements, clinical benefits could justify the effective dose from CBCT scanners. Further studies with more observers and newer CBCT machines available in the market are necessary to determine if results would improve. Based on the results of the current study, it is concluded that (1) there is a difference between cone beam computed tomography and conventional radiography for periodontal bone height detection (2) considerable differences occur between observers in the both modalities.

Table 1. Distribution of sample sites by tooth group, site location and amount of bone loss (see text for explanation of symbols).

	< 3 mm							≥ 3 mm						
	MB	B	DB	DL	L	ML	total	MB	B	DB	DL	L	ML	total
LA	0	5	4	2	1	0	12	0	5	4	0	3	0	12
LM	0	8	3	1	0	0	12	2	2	3	0	3	1	11
LP	0	8	4	0	0	0	12	3	3	2	0	3	1	12
UA	0	5	2	3	2	0	12	0	8	4	1	1	0	14
UM	0	9	3	0	0	0	12	0	2	3	3	4	0	12
UP	0	9	3	0	1	0	13	1	5	2	1	3	0	12
total	0	44	19	6	4	0	73	6	25	18	5	17	2	73
%total	0.0	60.3	26.0	8.2	5.5	0.0	100.0	8.2	34.2	24.7	6.8	23.3	2.7	100.0

Table 2. Bone loss detection accuracy as measured by A_z (ROC analysis) for each modality and tooth group. Homogeneous subsets for all data based on Tukey's HSD post-hoc test.

Modality	Tooth Group	Mean A_z	SD	Homogeneous Subsets
CBCT	Molar	0.82	0.14	A
	Premolar	0.79	0.07	A
	Anterior	0.59	0.06	B
FMX	Molar	0.45	0.06	B
	Premolar	0.52	0.11	B
	Anterior	0.46	0.08	B

CBCT = Cone-beam computed tomography; FMX = full-mouth series.

Table 3. Absolute differences between ground truth measurements and image measurements by modality and tooth group. Homogeneous subsets by modality based on Tukey's HSD post-hoc test

		UM	UP	UA	LM	LP	LA	pooled
CBCT	Mean	1.14	0.91	1.46	1.00	1.16	1.95	1.27
	SD	1.38	0.75	1.63	1.11	1.31	1.89	1.43
Homogeneous subsets		A,B	A	B	A,B	A,B	C	
FMX	Mean	1.38	1.22	1.48	1.16	1.48	2.24	1.49
	SD	0.98	0.91	1.24	0.98	1.11	1.78	1.24
Homogeneous subsets		A	A	A	A	A	B	
CBCT = Cone-beam computed tomography; FMX = full-mouth series.								

Table 4. Kappa values for intra-observer agreement between repeated ROC scores from bone loss assessment

Observer	CBCT	FMX
1	0.13	0.00
2	0.15	0.22
3	-0.17	-0.05
4	0.34	0.32
5	0.32	0.30
6	0.11	-0.05
Pooled	0.15	0.14
CBCT = Cone-beam computed tomography; FMX = full-mouth series.		

Table 5. Area under the ROC-curve (A_z) by modality, observer and tooth group (CBCT = Cone-Beam CT; FMX = full-mouth series)

Observer	Tooth group	CBCT		FMX	
		A_z	S.E	A_z	S.E
1	Molar	0.683	0.084	0.507	0.092
	Premolar	0.858	0.056	0.642	0.086
	Anterior	0.604	0.083	0.562	0.092
2	Molar	0.938	0.040	0.451	0.100
	Premolar	0.843	0.060	0.449	0.098
	Anterior	0.516	0.085	0.384	0.091
3	Molar	0.622	0.086	0.369	0.089
	Premolar	0.705	0.075	0.570	0.095
	Anterior	0.610	0.081	0.424	0.103
4	Molar	0.911	0.053	0.432	0.099
	Premolar	0.794	0.069	0.427	0.093
	Anterior	0.684	0.088	0.442	0.121
5	Molar	0.906	0.050	0.533	0.116
	Premolar	0.842	0.067	0.400	0.113
	Anterior	0.553	0.085	0.399	0.130
6	Molar	0.881	0.052	0.434	0.090
	Premolar	0.696	0.080	0.653	0.085
	Anterior	0.605	0.082	0.564	0.093
	Mean	0.735	0.071	0.480	0.099

Table 6. Descriptive statistics for Actual and Absolute differences between Ground Truth and CBCT image measurement (Phase I)

	n	mean	sd	median	min	max
Actual	270	-.40	1.17	-0.29	-5.86	5.75
Absolute	270	0.85	0.90	0.59	.00	5.86
Absolute difference: $p < 0.05$						

Table 7. Results of ANOVA statistics on actual differences between ground truth and CBCT image measurements

Source	Sum of Squares	F Ratio	Pro > F
Skull	17.39	6.676	<.0001
Tooth Group	31.08	9.5418	<u><.0001</u>
Site	2.93	8987	0.4825

Table 8. Results of ANOVA statistics on Az values

Source	N parm	DF	Sum of Squares	F Ratio	Prob > F
Observer	5	5	0.034	0.616	0.688
Tooth group	2	2	0.118	5.295	0.011
Modality	1	1	0.585	52.582	<u><0.0001</u>

Table 9. Summary of average differences between ground truth measurements and CBCT, FMX measurements (CBCT = Cone-Beam CT; FMX = full-mouth series)

Tooth group	CBCT		FMX	
	Mean	S.E	Mean	S.E
Anterior	-0.159	0.142	-1.156	0.114
Molar	-0.642	0.091	-0.886	0.083
Premolar	0.098	0.086	-1.081	0.079
Overall	-0.228	0.064	-1.171	0.054

Table 10. Tooth group wise distribution of absolute differences between CBCT and FMX modalities (CBCT = Cone-Beam CT; FMX = full-mouth series)

Tooth group	CBCT		FMX	
	Mean	S.E	Mean	S.E
Anterior	1.709	0.103	1.841	0.096
Molar	1.073	0.075	1.271	0.060
Premolar	1.031	0.062	1.348	0.061
Overall	1.276	0.049	1.485	0.044

Table 11. ANOVA results with significant interactions

Source	N parm	DF	Sum of Squares	F Ratio	Prob > F
Modality	1	1	545.95	184.19	<u><0.0001</u>
Observer	5	5	222.16	14.99	<u><0.0001</u>
Tooth group	5	5	91.70	6.19	<u><0.0001</u>
Site	5	5	60.95	4.11	0.0010
Observer * Modality	5	5	168.87	11.40	<u><0.0001</u>
Tooth group* Modality	5	5	111.23	7.59	<u><0.0001</u>

Table 12. Pearson correlation coefficients for ground truth and image measurements by modality and tooth group (*significant at $p < 0.05$)

Modality	UM	UP	UA	LM	LP	LA	pooled
CBCT	*0.31	*0.47	0.07	*0.39	*0.47	*0.16	*0.30
FMX	-0.25	0.17	-0.05	*0.41	0.06	0.00	0.06

Fig.1. Graph showing tooth group wise distribution of Absolute and Actual differences between CT and Ground truth measurements

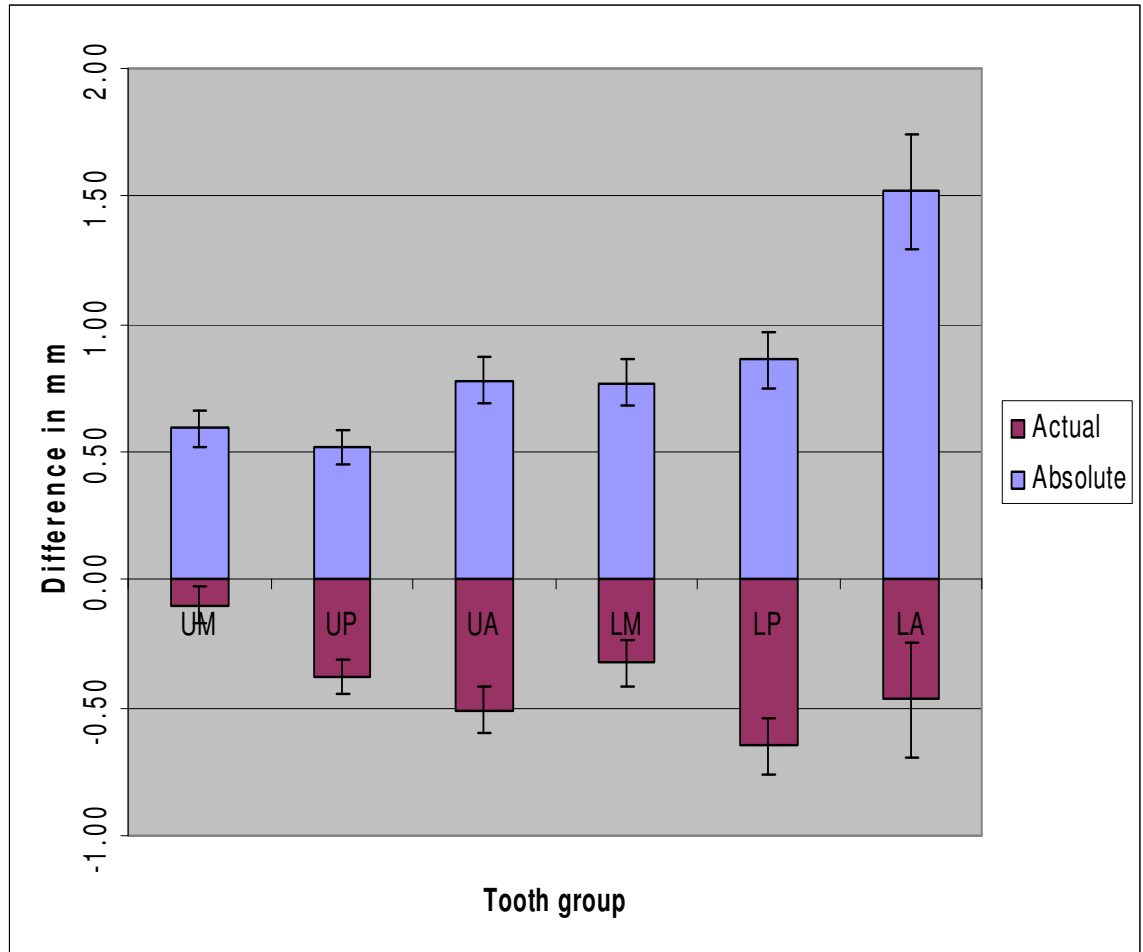


Fig.2. ROC curves for pooled A_z of two modalities (CBCT vs FMX) for detection for periodontal bone loss

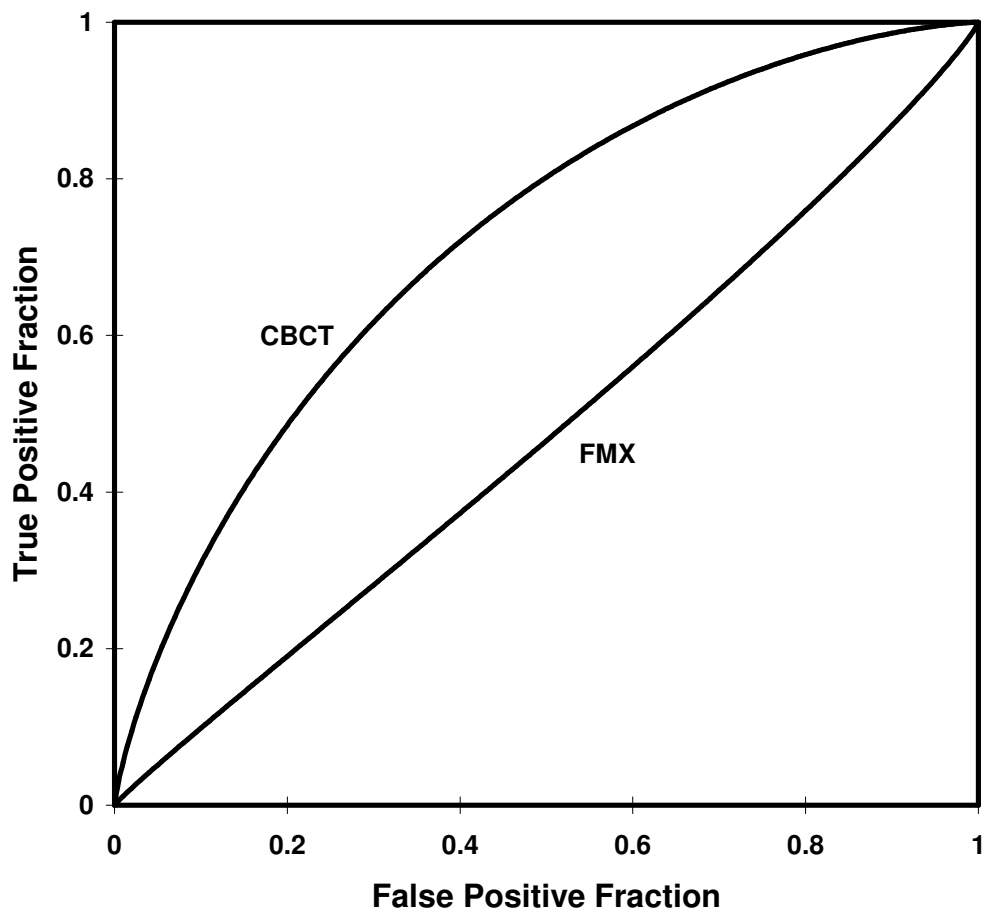


Fig.3. ROC curves for Molar, Premolar and Anterior tooth groups (Modality: CBCT)

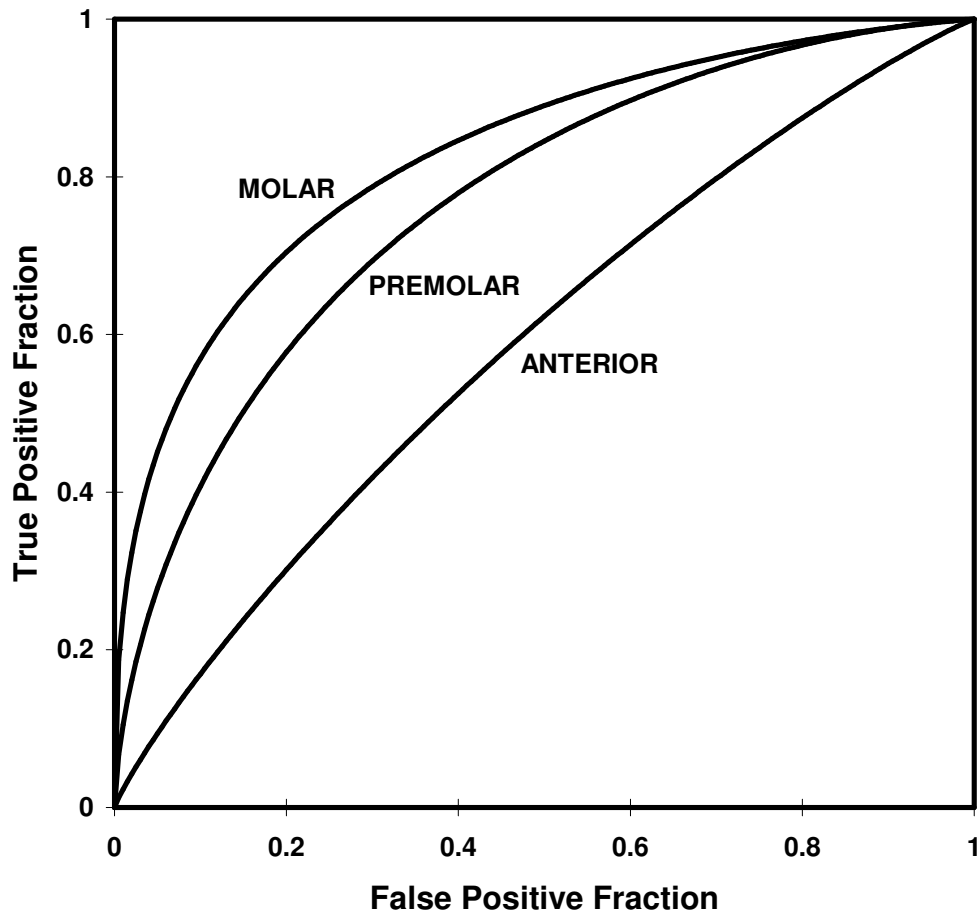


Fig. 4. ROC curves for Molar, Premolar and Anterior tooth groups (Modality: FMX)

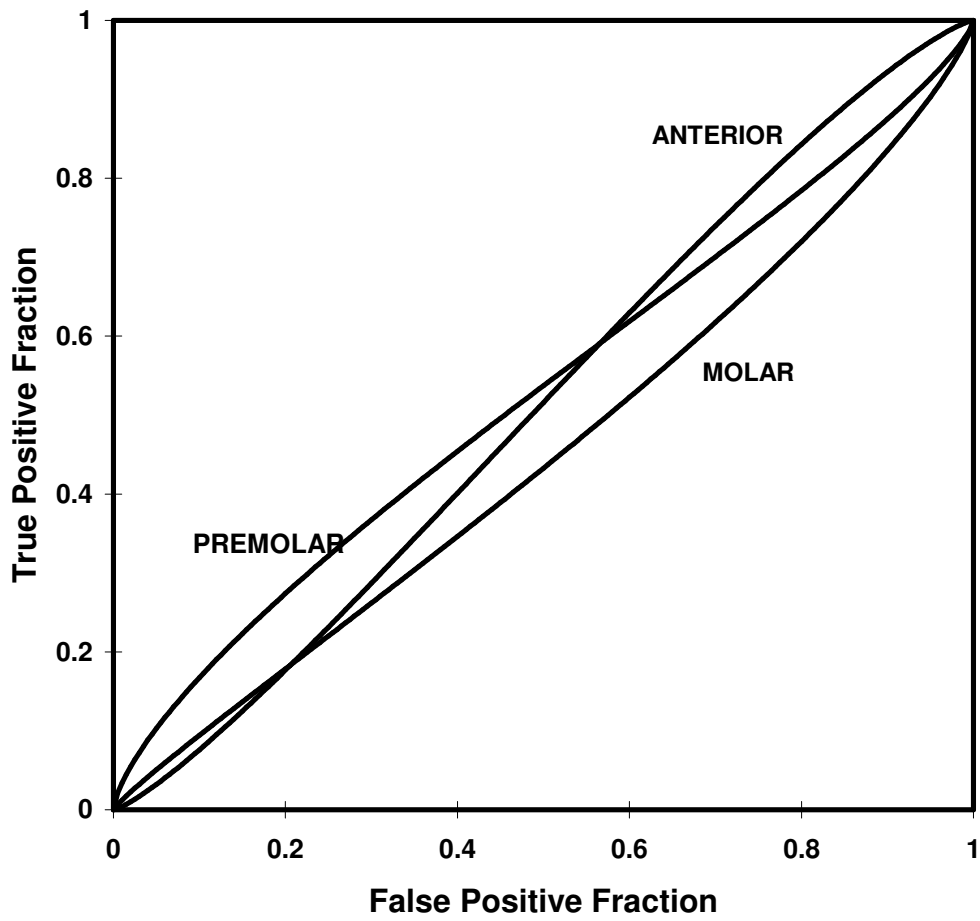


Fig. 5. Scatter plot with Pearson correlation for CBCT – Anterior tooth group

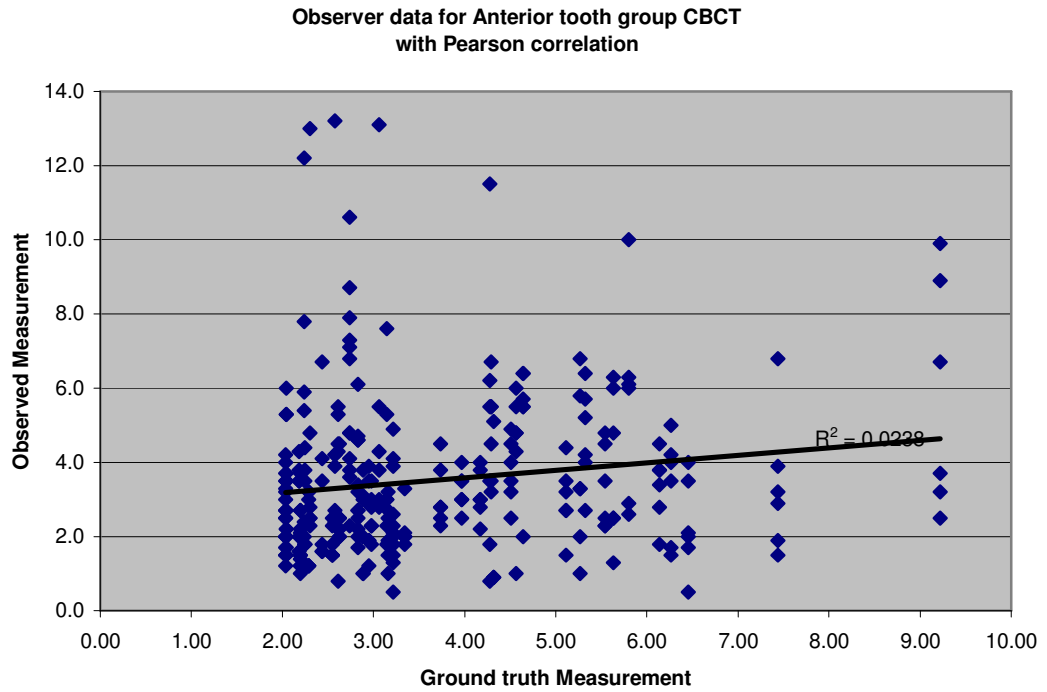


Fig. 6. Scatter plot with Pearson Correlation for FMX – Anterior tooth group

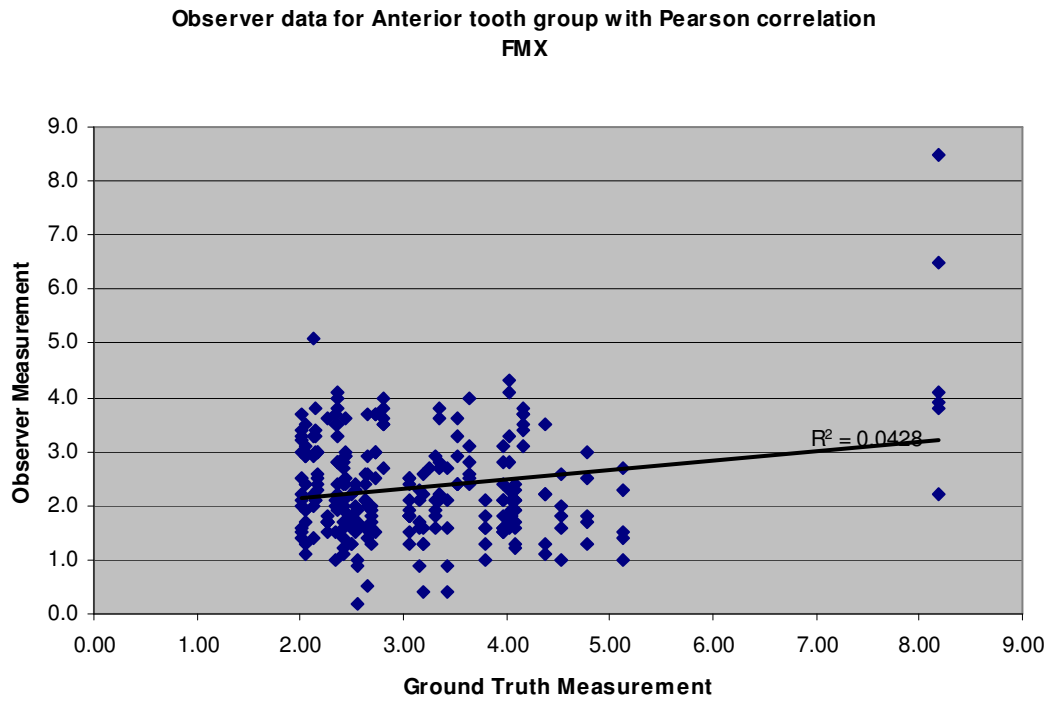


Fig. 7. Scatter plot with Pearson Correlation for CBCT – Molar tooth group

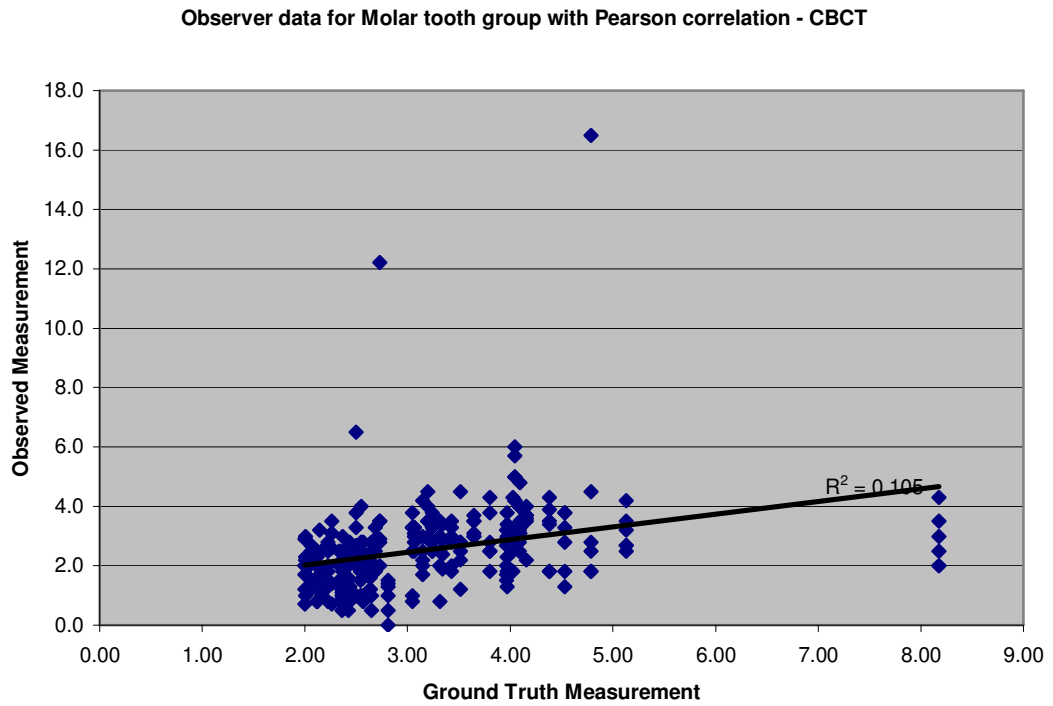


Fig. 8. Scatter plot with Pearson Correlation for FMX – Molar tooth group

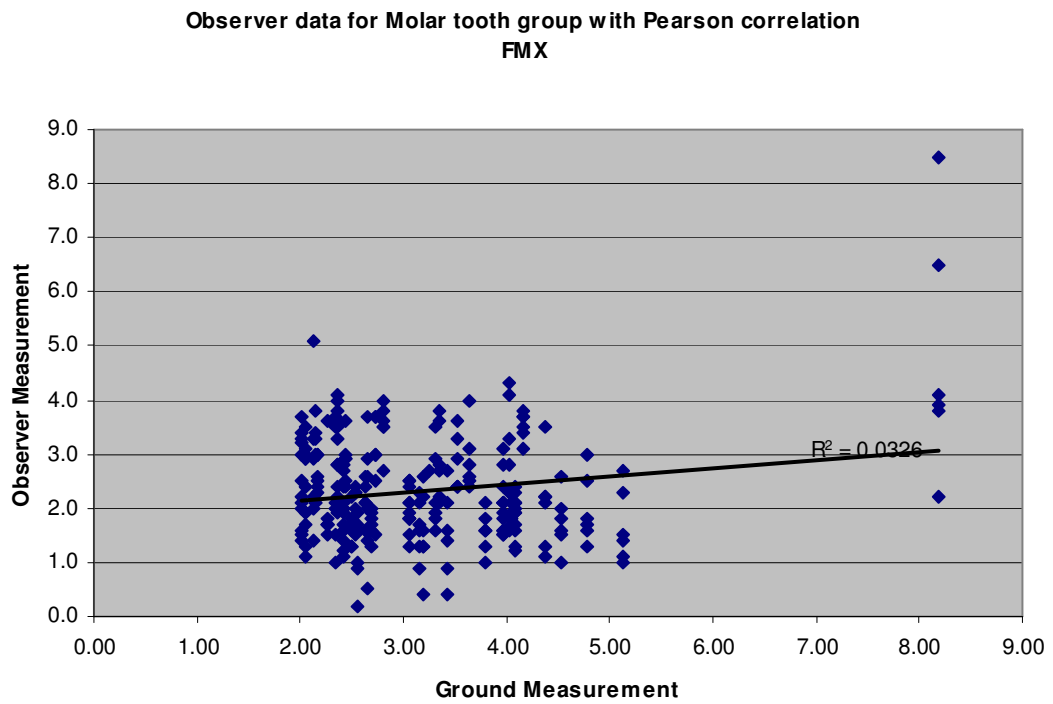


Fig. 9. Scatter plot with Pearson Correlation for CBCT – Premolar tooth group

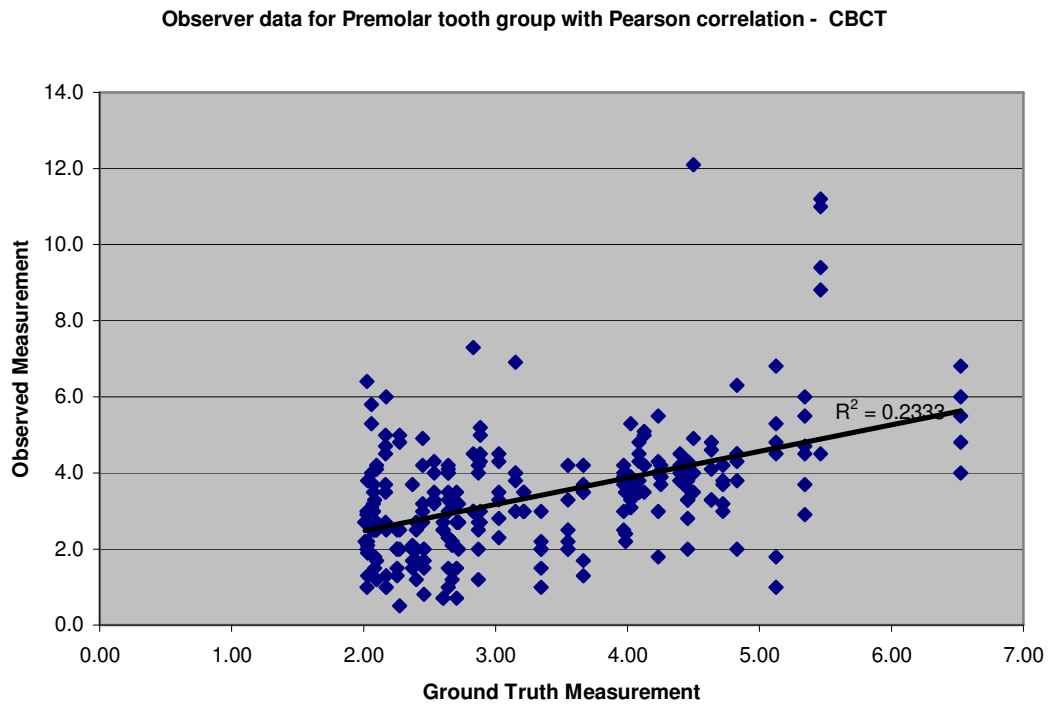


Fig. 10. Scatter plot with Pearson Correlation for CBCT – Premolar tooth group

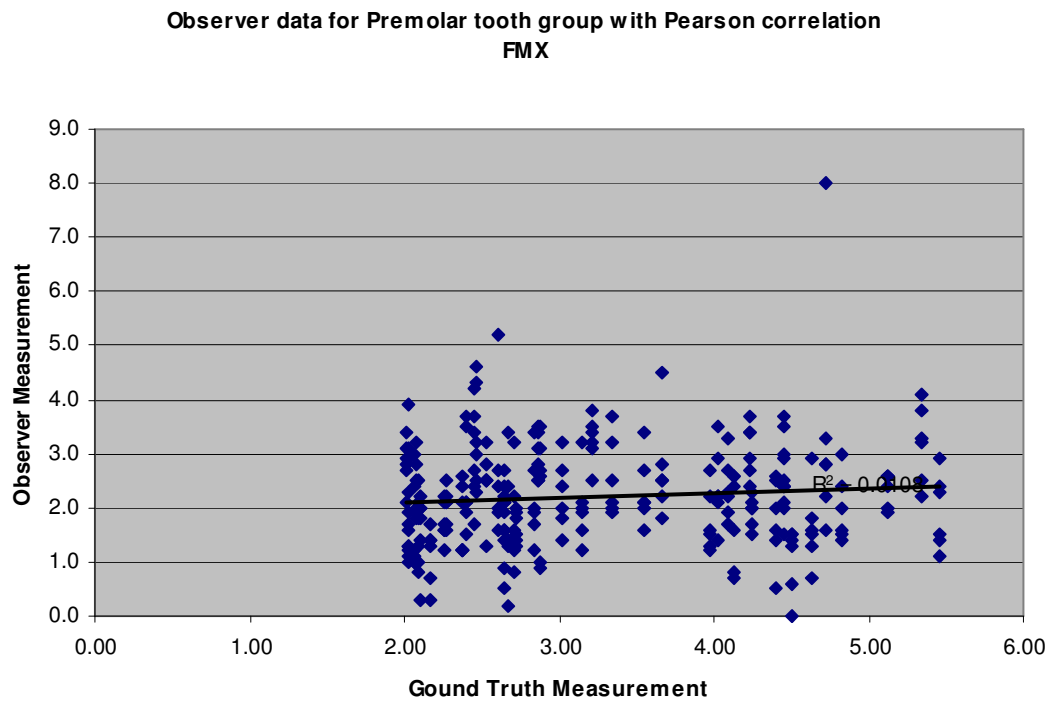


Fig.11.a. NewTom CBCT image slice of a lower lateral incisor (tooth #26) and B. corresponding incisor periapical radiograph (digital).



Fig. 12.a. NewTom CBCT image slice of a lower molar (tooth #31) and b. corresponding molar periapical radiograph (digital).

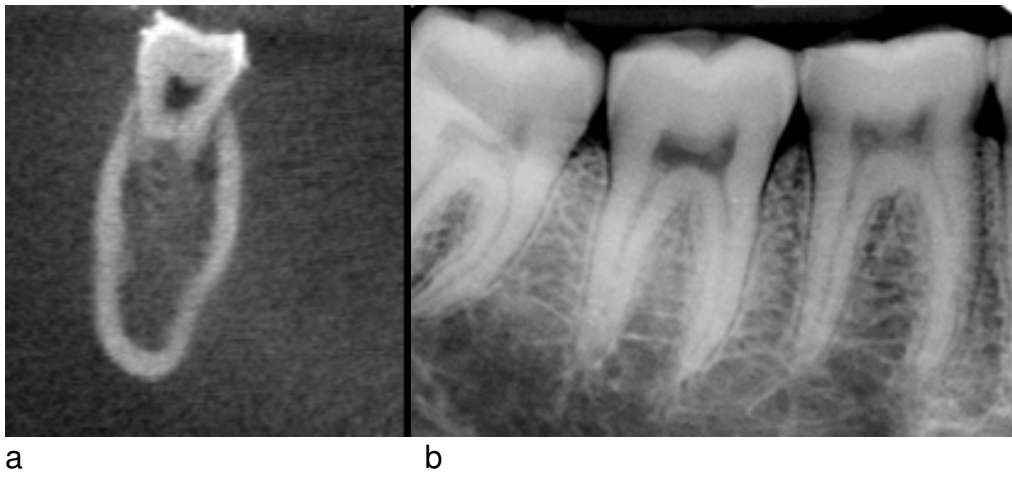
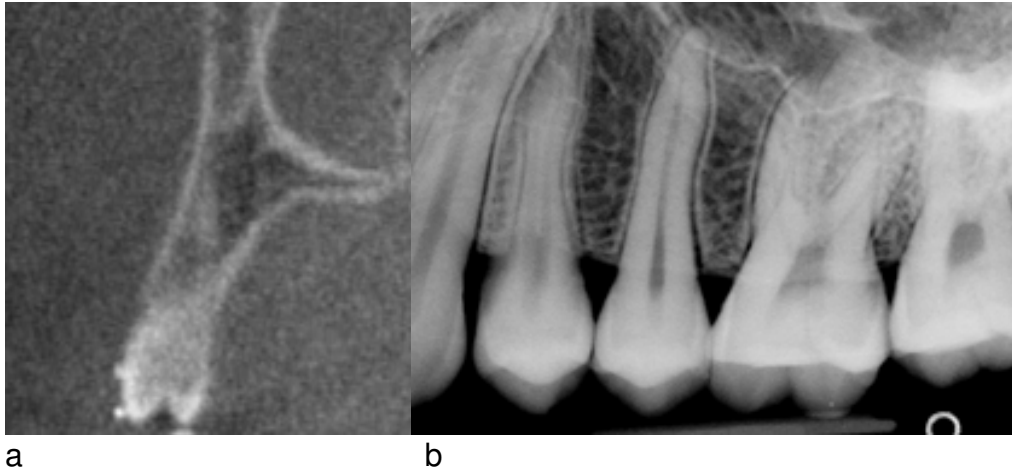


Fig.13.a. NewTom CBCT image slice of an upper premolar (tooth #13) and b. corresponding premolar periapical radiograph (digital).



References

1. Akesson, L., Hakansson, J., & Rohlin, M. (1992). Comparison of panoramic and intraoral radiography and pocket probing for the measurement of the marginal bone level. *Journal of Clinical Periodontology*, 19(5), 326-332.
2. Ames, J. R., Johnson, R. P., & Stevens, E. A. (1980). Computerized tomography in oral and maxillofacial surgery. *Journal of Oral Surgery (American Dental Association : 1965)*, 38(2), 145-149.
3. Araki, K., Maki, K., Seki, K., Sakamaki, K., Harata, Y., Sakaino, R., et al. (2004). Characteristics of a newly developed dentomaxillofacial X-ray cone beam CT scanner (CB MercuRay): System configuration and physical properties. *Dento Maxillo Facial Radiology*, 33(1), 51-59.
4. Armitage, G. C. (2004). Periodontal diagnoses and classification of periodontal diseases. *Periodontology 2000*, 34, 9-21.
5. Benn, D. K. (1992). A computer-assisted method for making linear radiographic measurements using stored regions of interest. *Journal of Clinical Periodontology*, 19(7), 441-448.
6. Cho, P. S., Johnson, R. H., & Griffin, T. W. (1995). Cone-beam CT for radiotherapy applications. *Physics in Medicine and Biology*, 40(11), 1863-1883.
7. Danforth, R. A., Dus, I., & Mah, J. (2003). 3-D volume imaging for dentistry: A new dimension. *Journal of the California Dental Association*, 31(11), 817-823.
8. Danforth, R. A., Peck, J., & Hall, P. (2003). Cone beam volume tomography: An imaging option for diagnosis of complex mandibular third molar anatomical relationships. *Journal of the California Dental Association*, 31(11), 847-852.
9. Davies, P. H., Downer, M. C., & Lennon, M. A. (1978). Periodontal bone loss in English secondary school children. A longitudinal radiological study. *Journal of Clinical Periodontology*, 5(4), 278-284.
10. Ekestubbe, A., Thilander, A., Grondahl, K., & Grondahl, H. G. (1993). Absorbed doses from computed tomography for dental implant surgery: Comparison with conventional tomography. *Dento Maxillo Facial Radiology*, 22(1), 13-17.
11. Fuhrmann, R. A., Bucker, A., & Diedrich, P. R. (1995). Assessment of alveolar bone loss with high resolution computed tomography. *Journal of Periodontal Research*, 30(4), 258-263.

12. Fuhrmann, R. A., Wehrbein, H., Langen, H. J., & Diedrich, P. R. (1995). Assessment of the dentate alveolar process with high resolution computed tomography. *Dento Maxillo Facial Radiology*, 24(1), 50-54.
13. Grondahl, H. G., & Grondahl, K. (1983). Subtraction radiography for the diagnosis of periodontal bone lesions. *Oral Surgery, Oral Medicine, and Oral Pathology*, 55(2), 208-213.
14. Grondahl, K., Grondahl, H. G., & Webber, R. L. (1984). Influence of variations in projection geometry on the detectability of periodontal bone lesions. A comparison between subtraction radiography and conventional radiographic technique. *Journal of Clinical Periodontology*, 11(6), 411-420.
15. Hansen, B. F., Gjermo, P., & Bergwitz-Larsen, K. R. (1984). Periodontal bone loss in 15-year-old Norwegians. *Journal of Clinical Periodontology*, 11(2), 125-131.
16. Hashimoto, K., Arai, Y., Iwai, K., Araki, M., Kawashima, S., & Terakado, M. (2003). A comparison of a new limited cone beam computed tomography machine for dental use with a multidetector row helical CT machine. *Oral Surgery, Oral Medicine, Oral Pathology, Oral Radiology, and Endodontics*, 95(3), 371-377.
17. Hatcher, D. C., Dial, C., & Mayorga, C. (2003). Cone beam CT for pre-surgical assessment of implant sites. *Journal of the California Dental Association*, 31(11), 825-833.
18. Hausmann, E. (1990). A contemporary perspective on techniques for the clinical assessment of alveolar bone. *Journal of Periodontology*, 61(3), 149-156.
19. Hausmann, E. (2000). Radiographic and digital imaging in periodontal practice. *Journal of Periodontology*, 71(3), 497-503.
20. Hausmann, E., Allen, K., Carpio, L., Christersson, L. A., & Clerehugh, V. (1992). Computerized methodology for detection of alveolar crestal bone loss from serial intraoral radiographs. *Journal of Periodontology*, 63(8), 657-662.
21. Herzog, A., & Paarmann, C. (1997). Enhancing accurate assessment of periodontal disease by improving radiographic interpretation. *Probe (Ottawa, Ont.)*, 31(4), 130-135.
22. Hull, P. S., Hillam, D. G., & Beal, J. F. (1975). A radiographic study of the prevalence of chronic periodontitis in 14-year-old English schoolchildren. *Journal of Clinical Periodontology*, 2(4), 203-210.
23. Jeffcoat, M. K., Wang, I. C., & Reddy, M. S. (1995). Radiographic diagnosis in periodontics. *Periodontology 2000*, 7, 54-68.

24. Kilic, A. R., Efeoglu, E., Yilmaz, S., & Orgun, T. (1998). The relationship between probing bone loss and standardized radiographic analysis. *Periodontal Clinical Investigations : Official Publication of the Northeastern Society of Periodontists*, 20(1), 25-32.
25. Kobayashi, K., Shimoda, S., Nakagawa, Y., & Yamamoto, A. (2004). Accuracy in measurement of distance using limited cone-beam computerized tomography. *The International Journal of Oral & Maxillofacial Implants*, 19(2), 228-231.
26. Ludlow, J. B., Davies-Ludlow, L. E., & Brooks, S. L. (2003). Dosimetry of two extraoral direct digital imaging devices: NewTom cone beam CT and Orthophos plus DS panoramic unit. *Dento Maxillo Facial Radiology*, 32(4), 229-234.
27. Mol, A. (2004). Imaging methods in periodontology. *Periodontology 2000*, 34, 34-48.
28. Mozzo, P., Procacci, C., Tacconi, A., Martini, P. T., & Andreis, I. A. (1998). A new volumetric CT machine for dental imaging based on the cone-beam technique: Preliminary results. *European Radiology*, 8(9), 1558-1564.
29. Naito, T., Hosokawa, R., & Yokota, M. (1998). Three-dimensional alveolar bone morphology analysis using computed tomography. *Journal of Periodontology*, 69(5), 584-589.
30. Oliver, R. C., Brown, L. J., & Loe, H. (1998). Periodontal diseases in the united states population. *Journal of Periodontology*, 69(2), 269-278.
31. Ortman, L. F., Dunford, R., McHenry, K., & Hausmann, E. (1985). Subtraction radiography and computer assisted densitometric analyses of standardized radiographs. A comparison study with 125I absorptiometry. *Journal of Periodontal Research*, 20(6), 644-651.
32. Pepelassi, E. A., & Diamanti-Kipioti, A. (1997). Selection of the most accurate method of conventional radiography for the assessment of periodontal osseous destruction. *Journal of Clinical Periodontology*, 24(8), 557-567.
33. Pistorius, A., Patrosio, C., Willershausen, B., Mildemberger, P., & Rippen, G. (2001). Periodontal probing in comparison to diagnosis by CT-scan. *International Dental Journal*, 51(5), 339-347.
34. Ramesh, A., Ludlow, J. B., Webber, R. L., Tyndall, D. A., & Paquette, D. (2001). Evaluation of tuned aperture computed tomography (TACT) in the localization of simulated periodontal defects. *Dento Maxillo Facial Radiology*, 30(6), 319-324.

35. Rothman, S. L., Chafetz, N., Rhodes, M. L., & Schwarz, M. S. (1988). CT in the preoperative assessment of the mandible and maxilla for endosseous implant surgery. work in progress. *Radiology*, 168(1), 171-175.
36. Schulze, D., Heiland, M., Thurmann, H., & Adam, G. (2004). Radiation exposure during midfacial imaging using 4- and 16-slice computed tomography, cone beam computed tomography systems and conventional radiography. *Dento Maxillo Facial Radiology*, 33(2), 83-86.
37. Sukovic, P. (2003). Cone beam computed tomography in craniofacial imaging. *Orthodontics & Craniofacial Research*, 6 Suppl 1, 31-6; discussion 179-82.
38. Tsiklakis, K., Syriopoulos, K., & Stamatakis, H. C. (2004). Radiographic examination of the temporomandibular joint using cone beam computed tomography. *Dento Maxillo Facial Radiology*, 33(3), 196-201.
39. Tugnait, A., Clerehugh, V., & Hirschmann, P. N. (2000). The usefulness of radiographs in diagnosis and management of periodontal diseases: A review. *Journal of Dentistry*, 28(4), 219-226.
40. Van der Stelt, P. F. (1993). Modern radiographic methods in the diagnosis of periodontal disease. *Advances in Dental Research*, 7(2), 158-162.
41. Vannier, M. W. (2003). Craniofacial computed tomography scanning: Technology, applications and future trends. *Orthodontics & Craniofacial Research*, 6 Suppl 1, 23-30; discussion 179-82.
42. Webber, R. L., Horton, R. A., Tyndall, D. A., & Ludlow, J. B. (1997). Tuned-aperture computed tomography (TACT). theory and application for three-dimensional dento-alveolar imaging. *Dento Maxillo Facial Radiology*, 26(1), 53-62.
43. Webber, R. L., & Messura, J. K. (1999). An in vivo comparison of diagnostic information obtained from tuned-aperture computed tomography and conventional dental radiographic imaging modalities. *Oral Surgery, Oral Medicine, Oral Pathology, Oral Radiology, and Endodontics*, 88(2), 239-247.
44. White, S. C. (1992). 1992 assessment of radiation risk from dental radiography. *Dento Maxillo Facial Radiology*, 21(3), 118-126.
45. White, S. C., & Pharoah, M. J. (2004). *Oral radiology : Principles and interpretation*. St. Louis, Mo.: Mosby.
46. Benn, D. K. (1992). A computer-assisted method for making linear radiographic measurements using stored regions of interest. *Journal of Clinical Periodontology*, 19(7), 441-448.

47. Fuhrmann, R. A., Bucker, A., & Diedrich, P. R. (1995). Assessment of alveolar bone loss with high resolution computed tomography. *Journal of Periodontal Research*, 30(4), 258-263.
48. Hausmann, E., & Allen, K. (1997). Reproducibility of bone height measurements made on serial radiographs. *Journal of Periodontology*, 68(9), 839-841.
49. Lascala, C. A., Panella, J., & Marques, M. M. (2004). Analysis of the accuracy of linear measurements obtained by cone beam computed tomography (CBCT-NewTom). *Dento Maxillo Facial Radiology*, 33(5), 291-294.
50. Pinsky, H. M., Dyda, S., Pinsky, R. W., Misch, K. A., & Sarment, D. P. (2006). Accuracy of three-dimensional measurements using cone-beam CT. *Dento Maxillo Facial Radiology*, 35(6), 410-416.